Fast size estimation of single-levitated nanoparticles in a vacuum optomechanical system: supplement

CUI-HONG LI,[1] JIANG JING,[1,2] LEI-MING ZHOU,[3] ZHEN-HAI FU,[1] XIAO-WEN GAO,[1] NAN LI,[1,2] XING-FAN CHEN,[1,2] AND HUI-ZHU HU[1,2,*]

[1]*Research Center for Quantum Sensing, Intelligent Perception Research Institute, Zhejiang Lab, Hangzhou 310000, China*
[2]*State Key Laboratory of Modern Optical Instrumentation, College of Optical Science and Engineering, Zhejiang University, Hangzhou 310027, China*
[3]*Department of Optical Science and Engineering, Hefei University of Technology, Hefei 230009, China*
*Corresponding author: huhuizhu2000@zju.edu.cn

Supplementary Material: Fast size estimation of single-levitated nanoparticles in a vacuum optomechanical system

CUI-HONG LI[1], JING JIANG[1,2], LEI-MING ZHOU[3], ZHEN-HAI FU[1], XIAO-WEN GAO[1], NANLI[1,2], XING-FAN CHEN[1,2], AND HUI-ZHU HU[1,2]

[1]Research Center for Quantum Sensing, Intelligent Perception Research Institute, Zhejiang Lab, Hangzhou, 310000, China.

[2]State Key Laboratory of Modern Optical Instrumentation, College of Optical Science and Engineering, Zhejiang University, Hangzhou, 310027, Zhejiang, China.

[3]Department of Optical Science and Engineering, Hefei University of Technology, Hefei, Anhui 230009, China.

1. Optical field distribution of the trapping beam

To gain the intensity I_0 of light illuminated on the levitated particle, the intensity distribution of the focused beam for trapping particles has been calculated. Fig. S1 illustrates the focusing of paraxial light beam by an aplanatic lens.
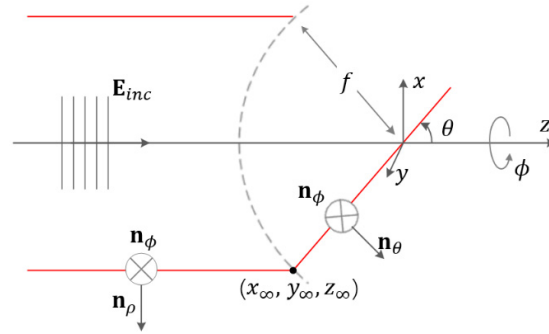
Figure S1: Geometric representation of an incident laser beam focused by an aplanatic lens system and definition of coordinates [1].

According to [1], the angular spectrum representation of a focal field can be expressed as

$$\mathbf{E}(\rho, \varphi, z) = -\frac{ikfe^{-ikf}}{2\pi} \int_0^{\theta_{max}} \int_0^{2\pi} \mathbf{E}_\infty(\theta, \phi) e^{ikz\cos\theta} e^{ik\rho\sin\theta\cos(\phi-\varphi)} \sin\theta d\phi d\theta$$

Where the definition of coordinates are denoted in Fig.S1, $\rho = \sqrt{x^2 + y^2}$, $k = nk_0 =$

$n\omega/c = n2\pi/\lambda$ represents wave number, f is focal length, $\mathbf{E}_\infty(\theta, \phi)$ is the field distribution on the reference sphere, the maximum angel θ_{max} is related to NA of the lens $\theta_{max} = \arcsin(NA)$. Fig. S2 shows the intensity distribution in the X–Y plane and three axes simulated with Debye integral. By fitting the intensity along each axis with Gaussian function, we get the $1/e^2$ intensity radius $\omega_X = 746\ nm$, $\omega_Y = 746\ nm$ and $\omega_z = 1576\ nm$.
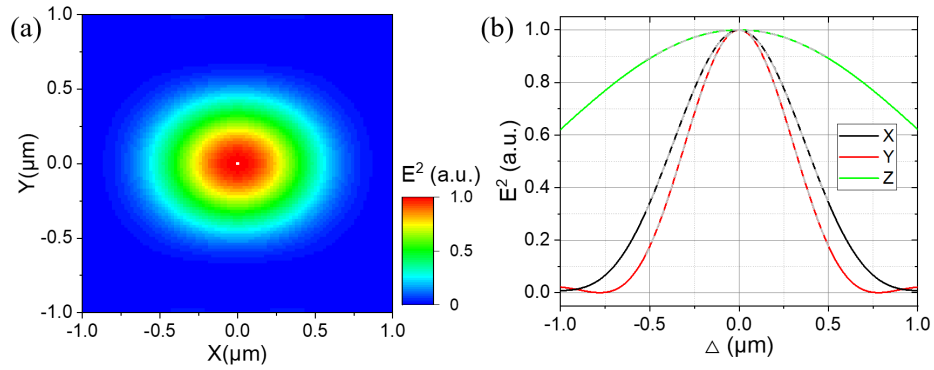

Figure S2: (a) The intensity distribution simulated with Debye integral in the X-Y plane. (b) Simulated intensity distributions along the X (blue) Y (red) and Z (green) axes. The dashed lines are fittings with a Gaussian function.

2. Scattering light detected by CMOS camera

The trapping laser beam introduces stray light easily inside the vacuum chamber. To distinguish with stray light, a CMOS camera is used to filter the particle scattering light. Fig. S3(a) shows the optical well imaged with the collecting system shown in Fig. 1(a) where objective lens and collective lens scatter significant light power. Fig. S3(b) illustrate that the scattered light from the trapped single nanoparticle is screened out by appropriate integration area selecting.
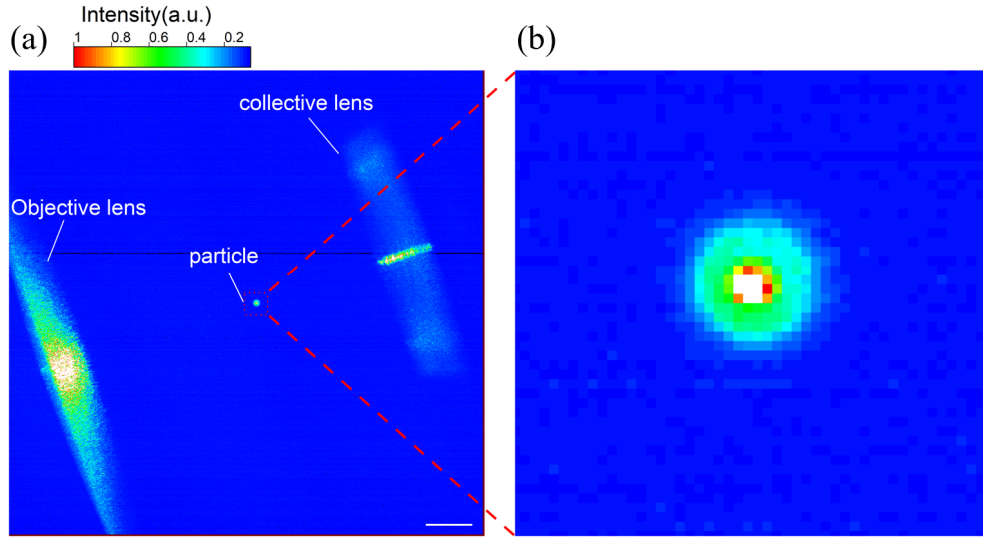
Figure S3: (a) Optically detected optical well on the CMOS camera. (b) Enlarged picture of trapped particle showing the light intensity integration area.

3. Experimental data of the 25 trapping experiments

In total, 25 trapping experiments is executed to confirm that the optically levitated single nano-spheres can be distinguished at ambient condition according to its scattering light. Table S1 lists the scattering light power collected in each trapping experiment; Particle radii calculated through scattering power and damping rate at 10 mbar is shown; The last column records whether the trapped particle can survive at low air pressure of 10^{-2} mbar or not. Fig. S4 shows the PSD of the motion of the No.10 particle at 5×10^{-3} mbar, which reveals that the particle survives in near high vacuum. The broadening of the resonance peaks of all three axes arises from thermal nonlinearities of the nanomechanical oscillator [2,3,4], which can be mitigated by feedback cooling.

Table S1: Experimental data of 25 trapped particles.

No.	$P_{scatter}$ (nW)	$R_{scatter}$ (nm)	$R_{damping}$X/Y/Z (nm)	Surviveness
1	9.69(0.26)	48.5	——	N
2	1.77(0.21)	36.5	——	N
3	45.54(0.37)	63	65.72(2.598)/65.28(2.651)/65.5(1.78)	Y

| 4	168.54(0.79)	78.5	76.66(2.622)/70.89(2.57)/78.58(3.076)	Y
5	88.81(0.33)	70	76.37(4.01)/76.58(3.106)/77.1(3.653)	Y
6	44.46(0.30)	63	67.29(2.122)/68.3(2.762)/68.7(2.694)	Y
7	307.27(1.28)	87	-/70.08(3.199)/70.54（3.311）	N
8	8.4(0.23)	47.5	——	N
9	107.94(0.56)	73	74.03(2.562)/58.73(2.2)/59.21(2.73)	Y
10	45.96(0.37)	63	66.85(3.254)/67.24(2.6)/67.51(3.021)	Y
11	275.3(2.5)	85	86.85(2.98)/69.64(2.46)/69(3.34)	Y
12	212.64(1.11)	82	82.9(3.24)/62.8(2.41)/64.4(2.16)	Y
13	310.14(0.89)	86.5	90(4.11)/71.8(3.61)/72(2.42)	N
14	152.68(0.97)	77	78.68(3.72)/65.6(3.44)/65.23(2.67)	Y
15	552.94(1.99)	95.5	97.85(4.07)/76.67(2.15)/75.49(3.34)	N
16	82.06(1.0)	69.5	70.8(2.41)/65.61(2.43)/66.41(1.85)	Y
17	179.01(1.2)	79	81.17(3.90)/65.28(2.58)/65.49(2.29)	Y
18	85.37(1.06)	70	63.52(2.46)/60.21(1.86)/63.53(2.82)	N
19	90.28(1.11)	70.5	71.83(3.25)/71.43(2.16)/72.24(3.12)	N
20	65.45(1.41)	60	57.81(2.32.)/55.89(1.69)/57.09(2.24)	Y
21	128.41(1.08)	68	69.16(3.52)/69.2(2.85)/67.96(2.83)	Y
22	54.32(0.93)	59	60.9(2.92)/61.62(2.66)/62.28(2.49)	Y
23	39.65(1.37)	56	71.84(2.56)/65.9(3.45)/67.86(2.61)	N
24	163.53(1.85)	70.5	67.24(2.77)/48.13(1.7)/58.89(1.49)	N
25	151.15(1.66)	69.5	70.22(2.4)/69.5(2.85)/69.56(3.01)	Y
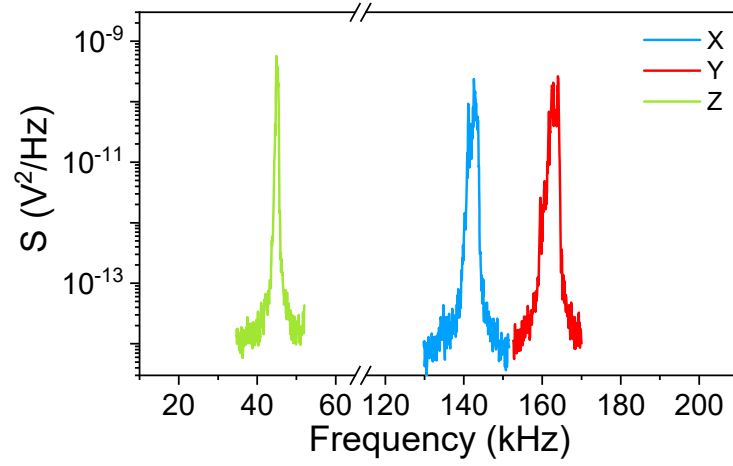
Figure S4: PSD motion signals of the particle along three axes at a pressure of 5×10^{-3} mbar.

4. Particle size

Two transmission electron microscope (TEM) images of the silica particles used in the experiment are displayed in Fig. S5. Statistical results on the 105 particles in the two pictures reviews that most of the particles have a diameter in the range of 100-200 nm as shown in Fig. S6. Thus, the single nanoparticle selection method sets particle radius selection range 50-100 nm.
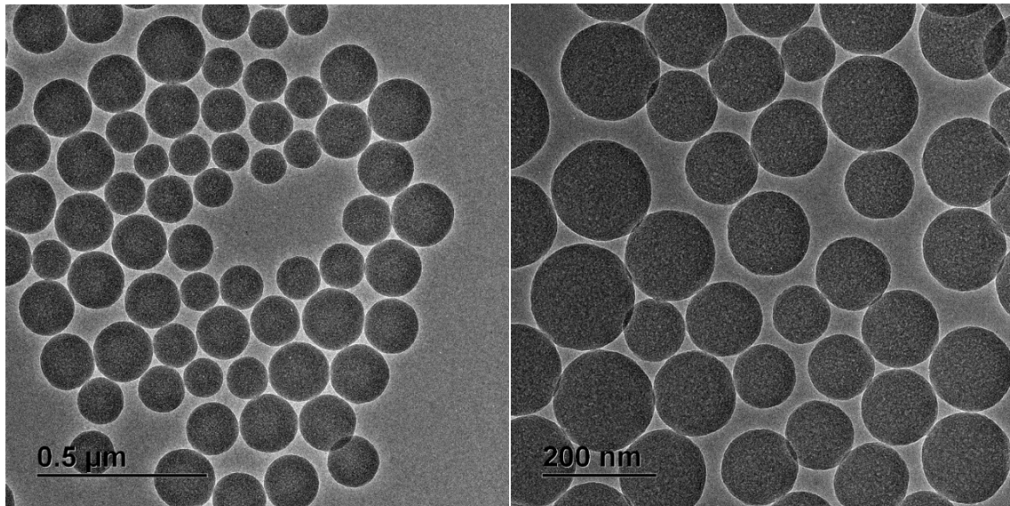

Figure S5: (a,b) TEM micrographs of the nano silica particles used in the experiment.
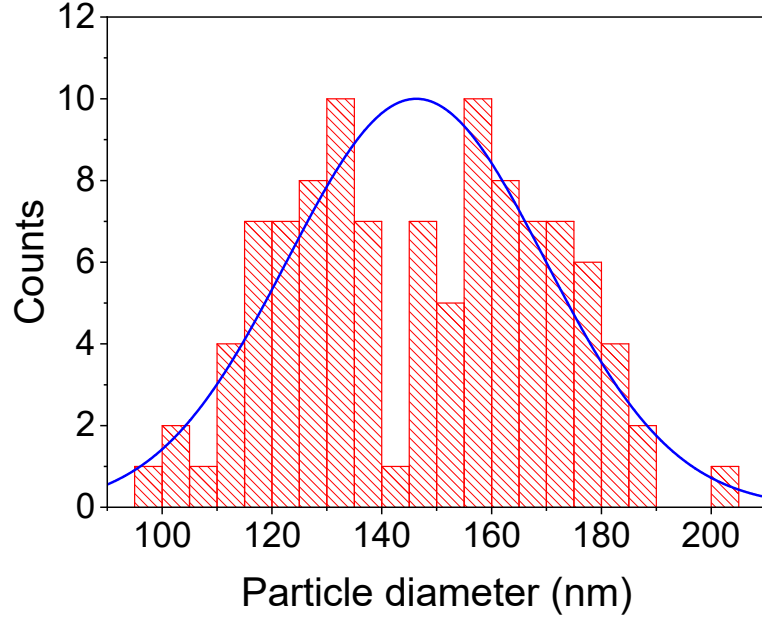
Figure S6: Statistical distribution of the nanoparticles

5. Criterion for single nanoparticles

According to Li at al.'s study [5], non-spherical particle like nanodumbbell (composed of two nanospheres) has different damping rates along three motion axes. Correspondingly, different radii values are calculated using the kinetic theory of particles in gas. To distinguish the calculated radii difference from particle composition and computational error, particle radii differences due to two reasons are analyzed.

A. Computational error of particle radii calculated based on the kinetic theory of particles in gas

Based on the kinetic theory of particles in gas, $\Gamma_0 = \frac{6\pi\eta R}{m} \times \frac{0.619}{0.619+k_n} \times (1+c_k)$ [6,7],

where $m = \frac{4}{3}\pi R^3, c_k = 0.31k_n/(0.785 + 1.152k_n + k_n^2), k_n = \frac{\bar{l}}{r}$,($\bar{l} = k_B T/\sqrt{2}\pi d_a^2 p$). At 10 mbar, $k_n \approx 145$, $ck \approx 0.002$. The radius of trapped particle is expressed:

$$R = 0.619 \times \frac{18\sqrt{2}\pi(d_a/2)^2\eta}{4K_B T\Gamma_0\rho} \times p$$

For the trapping and detection system used for analyzing the kinetic motion of particles in gas in our system, the error propagation on the calculation of radius R

gives:

$$\frac{\sigma R}{R} = \sqrt{\left(-\frac{\delta T}{T}\right)^2 + \left(-\frac{\delta \Gamma_0}{\Gamma_0}\right)^2 + \left(-\frac{\delta \rho}{\rho}\right)^2 + \left(\frac{\delta p}{p}\right)^2}$$

where $\frac{\delta T}{T} \approx 1\%$, $\frac{\delta \Gamma_0}{\Gamma_0} \approx 0.5\%$, $\frac{\delta \Gamma_0}{\Gamma_0} \approx 0.5\%$, $\frac{\delta \rho}{\rho} \approx 5-10\%$, $\frac{\delta p}{p} \approx 0.2\%$. The main error arises from material density. In 2020, Zheng et al. [2] demonstrated that the density of the silica particle produced by Bangs Laboratories (the same product catalog number to that used in our study) is $\rho = 2.01 \pm 0.10$ g/cm^3, correspondingly, $\frac{\delta \rho}{\rho} = 5\%$. The particle density we adopted is 2.0 kg/m^3 (product data sheet), which is 10% smaller than that of general amorphous silica. Thus, $\frac{\delta \rho}{\rho} = 5-10\%$.

Therefore, $\frac{\sigma R}{R} = 5.15 - 10.1\%$. Thus, in our study, Particle radii error 10% is accepted in our study.

B. Particle radii of a nanodumbbell composed of two nanospheres

In 2018, Li et al. [5] theoretically calculated and experimentally demonstrated that the damping rates of a nanodumbbell (composed of two nanospheres) moving along (Γ_X) and perpendicular (Γ_Y) to its axial direction has different values (Fig. S7). The calculated ratio is $\frac{\Gamma_Y}{\Gamma_X} = \frac{\Gamma_Z}{\Gamma_X} = 1.276$, when $\frac{L}{D} = 1.9$, and $\frac{\Gamma_Y}{\Gamma_X} = \frac{\Gamma_Z}{\Gamma_X} = 1.258$, when $\frac{L}{D} = 2$. Therefore, trapped particles that composed of more than one nanosphere can be distinguished through its difference in damping rates along different axes, as they tend to show damping anisotropy. Thus, their radii along each axis will be different according to the calculation model $\Gamma_0 = \frac{6\pi\eta R}{m} \times \frac{0.619}{0.619+k_n} \times (1+c_k)$ [6,7].
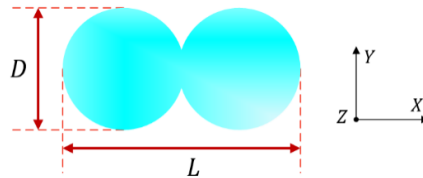

Figure S7: Schematic view of a nanodumbbell composed of two nanospheres.

For example, the trapped particle No. 9 has radii ratio of $\frac{R_X}{R_Y} = \frac{74.03 \ nm}{58.73 \ nm} = 1.26$, $\frac{R_X}{R_Z} = \frac{74.03 \ nm}{59.21 \ nm} = 1.25$. It is treated as non-single particles in the study.

Therefore, if the radii of the trapped particle calculated using kinetic theory has

difference of less than 10% along three axes and the radii is between 50-100nm (radii range of particle used in this study), we take the trapped particle as single particle.

To increase the ratio of single particles as much as possible, we highly dilute the particle suspension that nebulized and loaded in the optical trap. In our experiment, over half of the trapped particles selected as candidates of single nanoparticles through scattering power is verified using the kinetic theory, and the particle radii calculated using two methods match well. Moreover, it should be noted that if particle products with small radii range, like $SiO2$-R-L3205-21(143 ± 4 nm) nanoparticle product from Micro Particles, is used, we can directly tell if the particle is a single particle or not from its scattering power.

6. Phenomenon of particle adhering and loss in an optical trap

As a large number of droplets is introduced in the chamber in each particle nebulizing step, particle clusters can easily be introduced. What's worse, the number of captured particles frequently varies if the chamber is not evacuated quickly after particle capturing. Fig. S8 shows a trapping experiment in which the trapped particle passes through several particle adhering and loss processes.
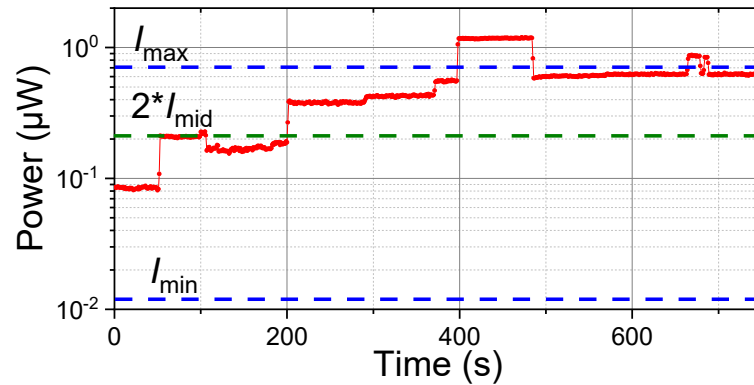

Figure S8: Scattered light of trapped particle under ambient condition recorded over a long duration with particle adhering and loss processes.

References

[1] Novotny, L. & Hecht, B. Principles of Nano-Optics (Cambridge University Press, 2006), 1st edn.

[2] Y. Zheng, L.-M. Zhou, Y. Dong, C.-W. Qiu, X.-D. Chen, G.-C. Guo, and F.-W. Sun, "Robust optical-levitation-based metrology of nanoparticle's position and mass," Phys. Rev. Lett. 124, 223603 (2020).

[3] J. Gieseler, L. Novotny, and R. Quidant, "Thermal nonlinearities in a nanomechanical oscillator," Nat. Phys. 9, 806–810 (2013).

[4] J. Gieseler, M. Spasenovic, L. Novotny, and R. Quidant, "Nonlinear mode coupling and synchronization of a vacuum-trapped nanoparticle," Phys. Rev. Lett. 112, 103603 (2014).

[5] J. Ahn, Z.-J. Xu, J. Bang, Y.-H. Deng, T. M. Hoang, Q.-K. Han, R.-M. Ma, and T.-C. Li," "Optically Levitated Nanodumbbell Torsion Balance and GHz Nanomechanical Rotor," Phys. Rev. Lett. 121, 033603 (2018).

[6] Y. Zheng and F. Sun, "Three-dimensional position measurement of a levitated nanoparticle in a vacuum by a dove prism," Chin. Opt. Lett. 17, 060901 (2019).

[7] S. Beresnev, V. Chernyak, and G. Fomyagin, "Motion of a spherical particle in a rarefied gas. part 2. drag and thermal polarization," J. Fluid Mech 219, 405–421 (1990).